



Environment Canada
Meteorological Service of Canada

Environnement Canada
Service météorologique du Canada

A Zeroth Order Lagrangian Particle Dispersion Model MLDP0

**Réal D'Amours
Alain Malo**

**Meteorological Service of Canada
Canadian Meteorological Centre
Environmental Emergency Response Section**

2004

1. INTRODUCTION

In the context of Lagrangian modeling, dispersion in the atmosphere is estimated by calculating the trajectories of a very large number of individual air particles (or parcels), in order to adequately « sample » the dispersing plume. These parcels are assumed to conserve their identity during their travel, but can transport some amount of tracer material which may be subject to various physical processes, like dry deposition, wet scavenging, and radioactive decay. If the 3-D wind field was completely specified at all points in space and all times, then calculating the trajectories would be the simple matter of solving the differential equation:

$$\frac{d\vec{r}}{dt} = \vec{V}(\vec{r}, t) \quad (1)$$

Usually a dispersion model is an « off-line » model, that is meteorological fields are provided by a Numerical Weather Analysis and Prediction System (NWP). These fields are available only at certain time intervals, and only at a limited number of discrete points in space. Therefore many scales of motion are not resolved. This is especially true of the turbulent components of the wind which are mostly responsible for the « mixing » of air parcels in the atmosphere. Fortunately, the information provided by the NWP systems can be used to estimate at least some the statistical properties of atmospheric turbulence.

Lagrangian Stochastic Models (LSM) use the statistical properties of atmospheric turbulence to model the mixing processes taking place in the atmosphere. These processes are usually called diffusion.

2. THE MODEL

LSM are based on the Langevin equation applied to particle velocities (Rodean, 1996). In the present model, vertical mixing is handled through a random displacement equation (equation 1) similar to the one used by Boughton et al. (1987). The random displacement equation (RDE) is the diffusion limit of the first order Langevin equation for stationary, inhomogeneous, Gaussian turbulence. Therefore, it is sometimes referred as a « zeroth » order model. The CMC model described here is called MLDP0 (*Modèle Lagrangien de Dispersion de Particules d'ordre 0*).

$$Z(t + \Delta t) = Z(t) + \left[\frac{\partial K_z}{\partial z} + w_s \right] \Delta t + \sqrt{2K_z} r, \quad r \in N(0, \sqrt{\Delta t}) \quad (2)$$

Boughton et al. (1987) have illustrated the equivalence of the Eulerian formulation of the gradient diffusion equation with the random displacement formulation.

In the equation above, K_z represents a vertical diffusion coefficient, w_s is the synoptic vertical motion, and r is a Gaussian random number with mean 0 and variance Δt .

As just noted the underlying assumption of the above RDE is Gaussian turbulence. The drift term (vertical gradient of K_z) is a result of that assumption. In order to have particles coming from above and from below a certain level with an equal probability, particles must have a tendency to drift away from a region with lower turbulence towards region of higher turbulence. Otherwise particles having a higher probability of large displacements in region of high turbulence (high diffusion coefficient K_z) would tend to accumulate in regions of low turbulence.

The main advantage of the RDE is that it allows for longer time steps than the discretized Langevin equation for particle velocities. However, relatively long discrete time steps can also lead into problems when K_z changes very rapidly in a quasi-discontinuous manner such as at the top of the atmospheric boundary layer or near the ground surface.

Near the ground particles that would experience a displacement below the ground (or below a certain reflection level close to the ground) are reflected upward. Particles that would experience a displacement above the ABL, because of the diffusion process, are reflected downward. Transport above the ABL due to synoptic vertical motion is allowed.

3. THE VERTICAL DIFFUSION COEFFICIENT

If the vertical diffusion coefficient K_z is available from NWP it can be readily used by MLDP0. However, this is not usually the case. It must therefore be calculated diagnostically from other meteorological variables.

Because of the reflection condition at the top of the ABL, the profile of K_z should be consistent with the depth of the ABL. For this reason it was decided to use a formulation that would mimic an ideal conceptual profile and the O'Brien (1970) was selected. Following Delage (1988), the height of the first level of the driving NWP model is taken as the height of the surface layer. K_z at this level is calculated in terms of a mixing length, stability function, and vertical wind shear, according to Delage (1997). The stability functions used depend on the Richardson number, and are identical to those used in CMC's Global Environmental Multiscale (GEM) model (Mailhot et al., 1998), see Appendix 1.

4. HORIZONTAL DIFFUSION

Lateral mixing is still an open question (Pudykiewicz and Koziol, 1998). In reality a good portion of the plume lateral spread can be accounted by the combined effect of vertical wind shear (e.g. the Ekman spiral) and vertical mixing in the boundary layer (Wilson and Sawford 1996). Nevertheless, it was found necessary to include a model for horizontal diffusion in MLDP0 in order to account for the effects of unresolved horizontal fluctuations of the mean wind in the boundary layer. This is sometimes referred to as plume meandering. This process is simulated with the first order Langevin equation shown below.

$$du_m = -\frac{u_m}{\tau_m} dt + \sqrt{\frac{2\sigma_{u_m}^2}{\tau_m}} R, R \in N(0, \sqrt{dt}) \quad (3)$$

The variance in the random term is based on GEM global analysis system verification statistics against radiosonde observations. Some of these statistics are shown in Table 1.

Table 1. Average variance of the wind differences between radiosonde observations and values obtained by the GEM global analysis system. The West-East (u) and South-North (v) are verified independently. O-A compares the observation with the Analyses, while O-F compares the observations with a 6-hour forecast (trial field)

| | O-A | | O-F | |
|---------|---------------------------------|---------------------------------|---------------------------------|---------------------------------|
| | $\sigma^2 u$ (m^2s^{-2}) | $\sigma^2 v$ (m^2s^{-2}) | $\sigma^2 u$ (m^2s^{-2}) | $\sigma^2 v$ (m^2s^{-2}) |
| 700 hPa | 2.2 | 2.1 | 8.1 | 7.4 |
| 850 hPa | 2.3 | 2.1 | 7.5 | 6.9 |

It is seen that for the analysis values (O-A) there is little difference between the 700 hPa and 850 hPa levels. Furthermore there is little difference -no anisotropy- between the U and V components. The O-F variances are significantly higher seem to be showing some anisotropy. Most likely forecast errors are present. Since there is no forecast errors associated with the O-A errors, one can assume that the variance of these errors represent the variance of the scales of motions not resolved by the Global Analysis System. Similar statistics are not available for the GEM regional analysis system. However verification of the regional GEM "0-Hour" forecast against radiosonde observations indicates similar "error" variances. There are no indications on the time scale at which these unresolved motions are effective, however it has been shown that mesoscale horizontal wind fluctuations have time scales of a few hours (Hanna, 1983). At this stage these statistics can only serve as a guide to an empirical determination of $\sigma_{u_m}^2$ and τ_m which should also include considerations based on model validation.

5. REMOVAL PROCESSES

In MLDPO a particle is assumed to represent the ensemble average of a large number of « real » particles. At the emission, it is assigned a mass which depends on the total quantity of material emitted and the total number of particles. The effect of radioactive decay, wet scavenging and dry deposition can be simulated by calculating the amount of material removed from the carrier particle, when it travels in regions of the atmosphere where such processes are active.

Dry deposition occurs when a particle is subjected to a reflection. It is modeled in term of a deposition velocity and an absorption probability. The absorption probability is calculated according to Wilson et al. (1989):

$$P = 1 - R; \quad R = \frac{1-a}{1+a}; \quad a = \left(\frac{\pi}{2}\right)^{\frac{1}{2}} \frac{v_d}{\sigma_w} \quad (4)$$

Where R is the reflection probability, v_d is the dry deposition velocity and σ_w the variance of the vertical turbulent wind component. Since σ_w is not usually available it is approximated in terms of the variance of the random vertical displacement, which according to the assumptions of RDE (eqn. 1) is given:

$$\overline{\Delta z^2} = 2K_z \Delta t, \quad \sigma_w \approx \frac{\sqrt{\overline{\Delta z^2}}}{\Delta t} = \sqrt{\frac{2K_z}{\Delta t}} \quad (5)$$

Since a particle represents the mean of an ensemble of particles, the fraction of the mass removed by dry deposition is equal to P .

Wet scavenging will occur when a particle is presumed to be in a cloud. The tracer removal rate is proportional to the local cloud fraction, and the particle mass.

6. CONCENTRATION CALCULATION

In MLDP0, tracer concentration at a given time and location are obtained by calculating the average residence time of the particles, during a given time period, within a given sampling volume, and weighing it according to the material amount carried by the particle. To obtain concentration fields, the sampling volumes become the set of boxes associated with the desired 3-D grid. See Appendix 2.

7. MODEL VALIDATION

ETEX

The European Tracer Experiment, ETEX, was conducted in the fall of 1994. The details of the experiment can be found in a special volume of Atmospheric Environment (van Dop et al., 1998). The Canadian Meteorological Centre participated in both the real time and the model inter-comparison phases of the experiment.

The first experiment in which 340 kg of an inert gas tracer was emitted for 12 hours started on October 23 1600 UTC. The release occurred at Monterfil in Western France. Measurements of the tracer concentration were performed over a network of 168 stations with a 3 hours time resolution for up to 90 hours after the start of the release.

Meteorological fields were obtained from a series of 3 and 6 hours forecasts by the GEM model in regional mode, at a resolution of about 15 km over Europe. These forecasts were initialized with the operational CMC global objective analyses available for that period. These meteorological fields were then used to run the MLDP0.

In order to be able to compare modeling results with observations 3-hour average concentrations were calculated at stations by using the method described in Appendix 2, with a cylindrical sampling volume 25 km in radius, and 100 m in height. Sampling time intervals were 900 seconds. These concentrations can be compared to the observations. Global statistics (see Appendix 3 for definitions) are presented in table 2. These statistics exclude station F21. The main reason is the fact that the station is situated at a distance of a little more than 21 km from the source. This implies that the source is within the sampling volume. Furthermore since meteorological data is available at a resolution of 15 km (and at time intervals of 3 hours) it was decided that this station is not adequate to evaluate the model performance. The next closest station in the path of the plume is over 160 km from the source, so all other stations are used in the statistics.

Table 2. *Global Scores (see Appendix 3) for the ETEX station network except station F21. Simulations were done up to 79 hours after the beginning of the release, and compared with observations. Results are given for different combinations of variances and time scales for the horizontal diffusion. Results are also given for cases where the vertical diffusion coefficient K_z is calculated with the ABL height H given by the GEM model (H-GEM). In the other cases K_z is estimated by the method given in Appendix 1.*

| σ_{um}^2 (m ² s ⁻²) | τ_m (s) | NMSE | BIAS | FB | PC | FMT | FA2 | FA5 |
|---|--------------|------|------|-----|-----|-----|-----|-----|
| 2.0 | 5400 | 14.4 | .05 | .46 | .58 | .32 | .23 | .47 |
| 2.0 | 10800 | 13.6 | .05 | .46 | .57 | .32 | .26 | .51 |
| 2.0 | 21600 | 13.1 | .05 | .45 | .57 | .33 | .27 | .53 |
| 3.0 | 5400 | 13.9 | .05 | .43 | .58 | .32 | .27 | .50 |
| 3.0 | 10800 | 12.9 | .05 | .43 | .57 | .33 | .28 | .54 |
| 3.0 | 21600 | 12.5 | .05 | .43 | .56 | .33 | .31 | .56 |
| 4.0 | 10800 | 10.9 | .05 | .45 | .58 | .34 | .29 | .55 |
| 3.0 (H-GEM) | 10800 | 16.2 | .07 | .54 | .61 | .36 | .29 | .56 |
| 4.0 (H-GEM) | 10800 | 14.9 | .07 | .54 | .61 | .36 | .30 | .57 |

From Table 2, it is seen that increasing the variance of the horizontal diffusion has the general effect of improving the scores slightly. This is also seen when the time scale is increased. Using the model ABL height results in slightly deteriorated NMSE and BIAS, however the other scores are somewhat better. There is a constant the tendency of the model to over estimate concentrations. Based on these results it was decided (more or less arbitrarily) to use $\sigma_{um}^2 = 3.0$ m²s⁻² and $\tau_m = 3$ hours as default values.

Figure 1 shows the position of a set of 10 stations disposed on two arcs across the path of the dispersing plume. In Figures 2 and 3, time series of modeled concentration values and observed values are presented for these stations. Generally the shape and the timing of plume passage are well reproduced. One can note that the model underestimate concentrations in the northern portion of the plume (e.g. NL 05, DK05), while there is an overestimation in the southern part (H02). The central part seems to be better handled (D05).

The model tendency is confirmed in Figures 4 and 5. Especially in Figure 4, it is seen that the tail end of the plume does not extend far enough to the southwest missing a few stations reporting fairly high concentrations. In Figure 5 the model produces a fairly large area of concentrations above 1 ng m^{-3} while according to the observations such an area is found only in the northern portion of the plume over Norway and Denmark.

The Algeciras Incident

The Algeciras incident provides another opportunity to validate the model. A biomedical device was accidentally processed in a foundry in Algeciras, Spain. It is estimated that about 50 Ci ($1.85\text{E}+12 \text{ Bq}$) of Cs-137 was released over a short period (~ 30 minutes) shortly after 00 UTC on May 30, 1998. The resulting plume, as it evolved over the next several days, was detected by several of the radionuclide monitoring stations over Europe.

Again in order to perform dispersion simulations, meteorological fields were obtained from a series of 3 and 6 hours forecasts by the GEM model in regional mode, at a resolution of about 30km over Europe. These forecasts were initialized with the operational CMC global objective analyses available for that period.

This being a real case, there is uncertainty about the source term. Furthermore, observations are not conveniently standardized. There is a fair amount of differences in sampling times and period, and most observations were taken over periods ranging from 3 to 10 days. A set of observations was assembled by ARAC and made available to the dispersion modeling community. In order to ensure inter-comparability observations were converted to time integrated concentrations.

In Figure 6, the time integrated surface concentration for an 8 day simulation can be compared with the observations. It can be seen that the main trunk of the plume is well depicted by the simulation. The axis of higher concentrations is well reproduced. The model indicates a splitting of the plume on each side of the Alps, which appears to be supported by the data. One can also see that there is a fair amount of variability in the observed concentrations in the mountainous terrain over Northern Italy. Such variability cannot be reproduced by the large scale model.

A few observations at a higher time resolution are available. At Ispra in Northern Italy daily average concentration have been measured. In Figure 7, these measurements can be compared with four MLDPO runs using various combinations of dry deposition velocities and wet scavenging ratios. Again the model reproduces well the timing of the plume passage, but the intensity is overestimated. Increasing the deposition velocity from $1 \text{ to } 3 \text{ mm s}^{-1}$ reduces significantly the overestimation. Variation in the wet scavenging coefficient has less effect. Again it must be emphasized, that Ispra is in the region where high horizontal variability is seen in the measurements, and that higher concentrations were measured in the vicinity.

8. CONCLUSION

MLDP0 was shown to produce credible simulations of large scale atmospheric dispersion. It is a simple and efficient model. An 80 hour simulation using 90k particles takes less than 20 minutes on a 20GHz pc, making it suitable for Environmental Emergency Response.

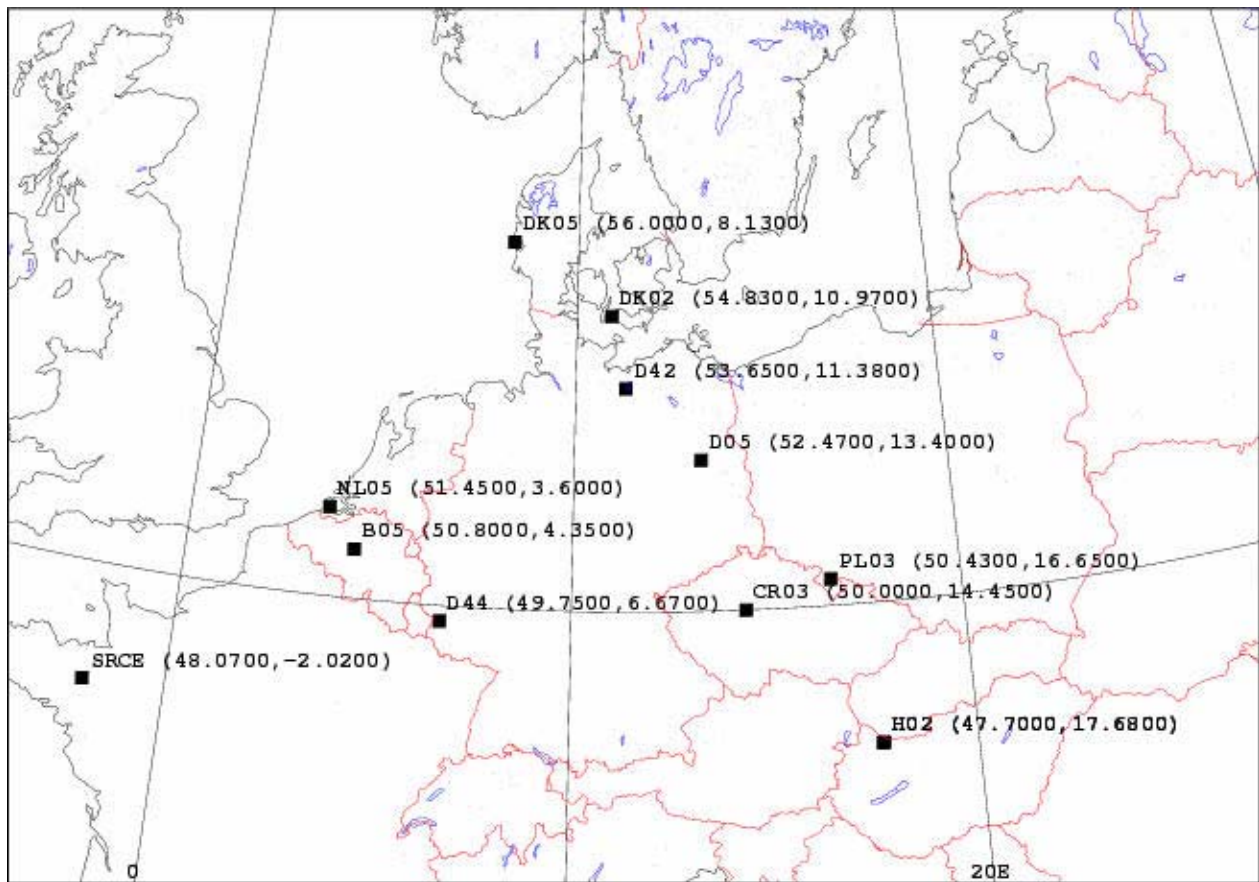


Figure 1. Position of selected stations for which time series have been produced in Figures 2 and 3. SRCE is the source of emission.

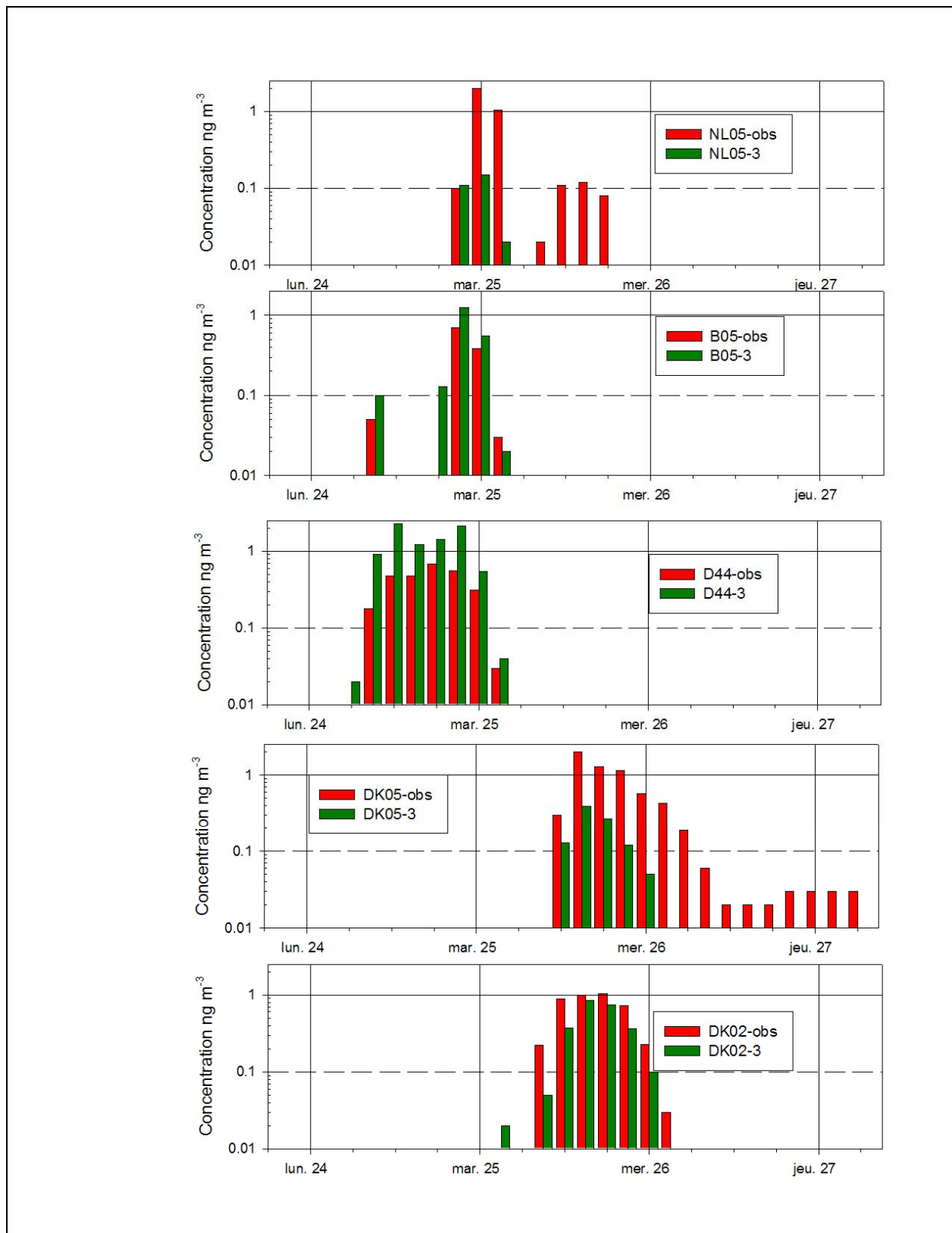


Figure 2. Time series of modeled surface concentrations compared to observations for 5 stations shown in Figure 1.

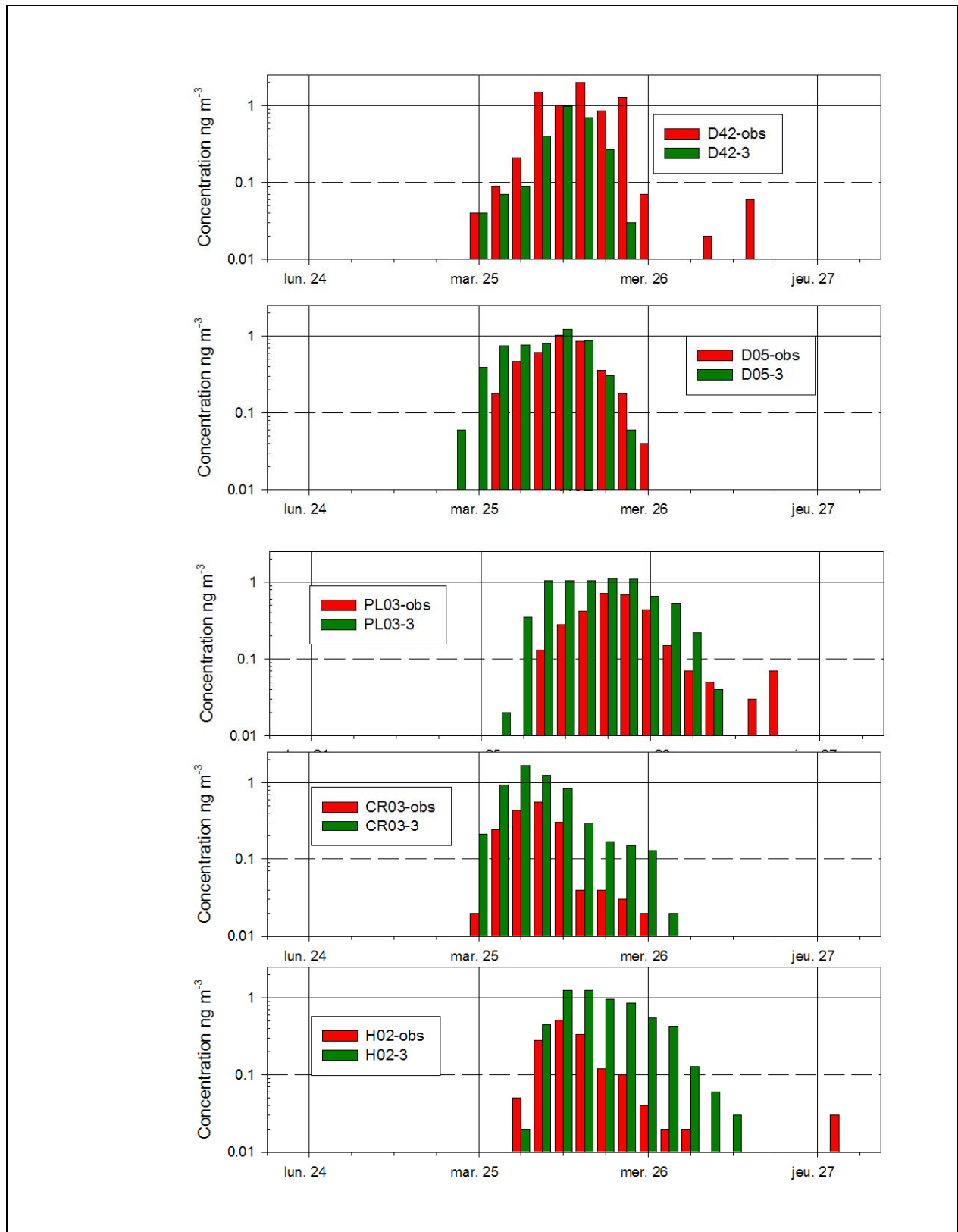


Figure 3. Time series of modeled surface concentrations compared to observations for the next 5 stations shown in Figure 1.

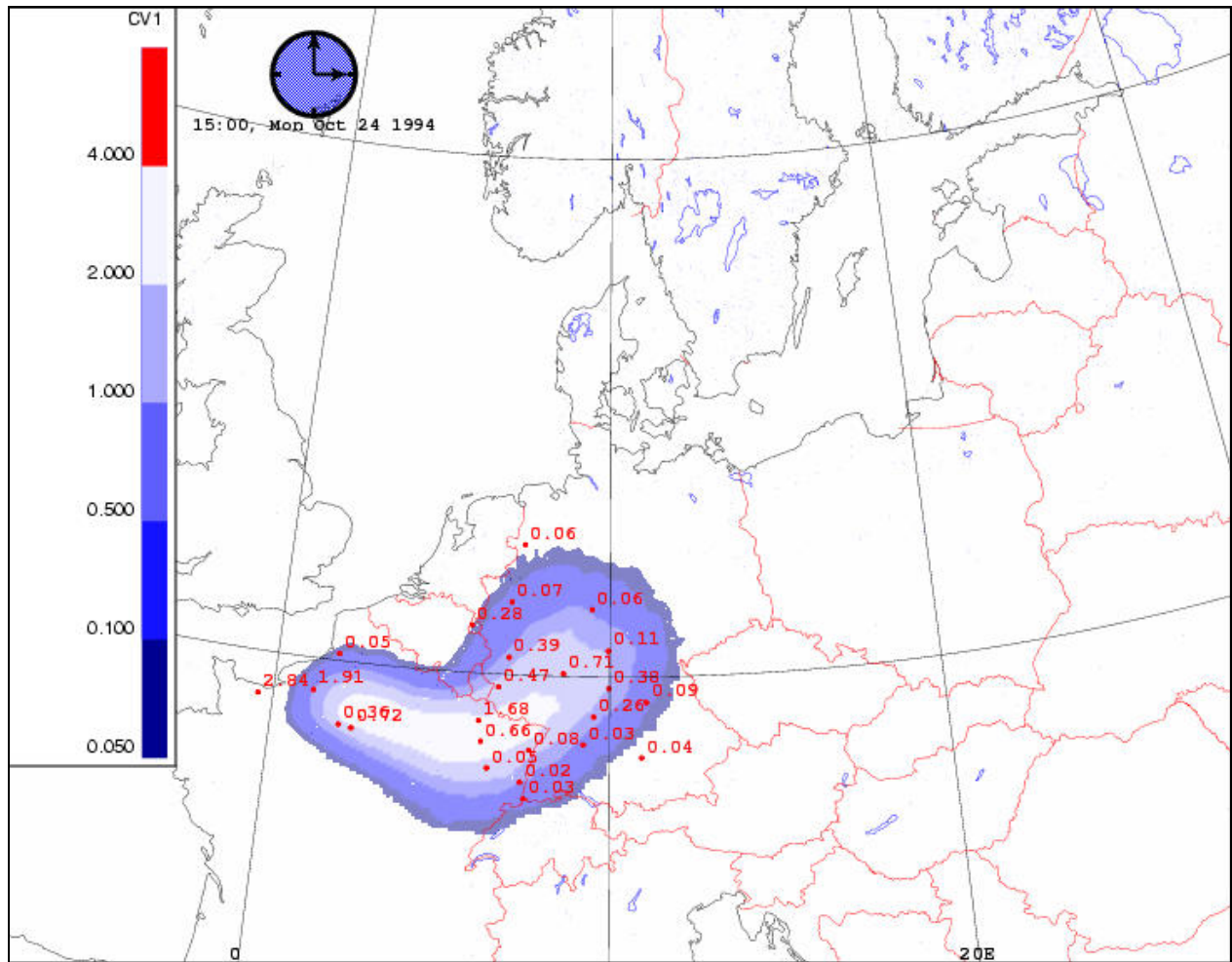


Figure 4. Plot of 3 hour average surface concentration valid at 1500 UTC 24 October 1994 (23 hours after the start of the release). The modeled plume can be compared to observations plotted in red. For clarity only positives reports are plotted. Zero concentration reports are not shown.

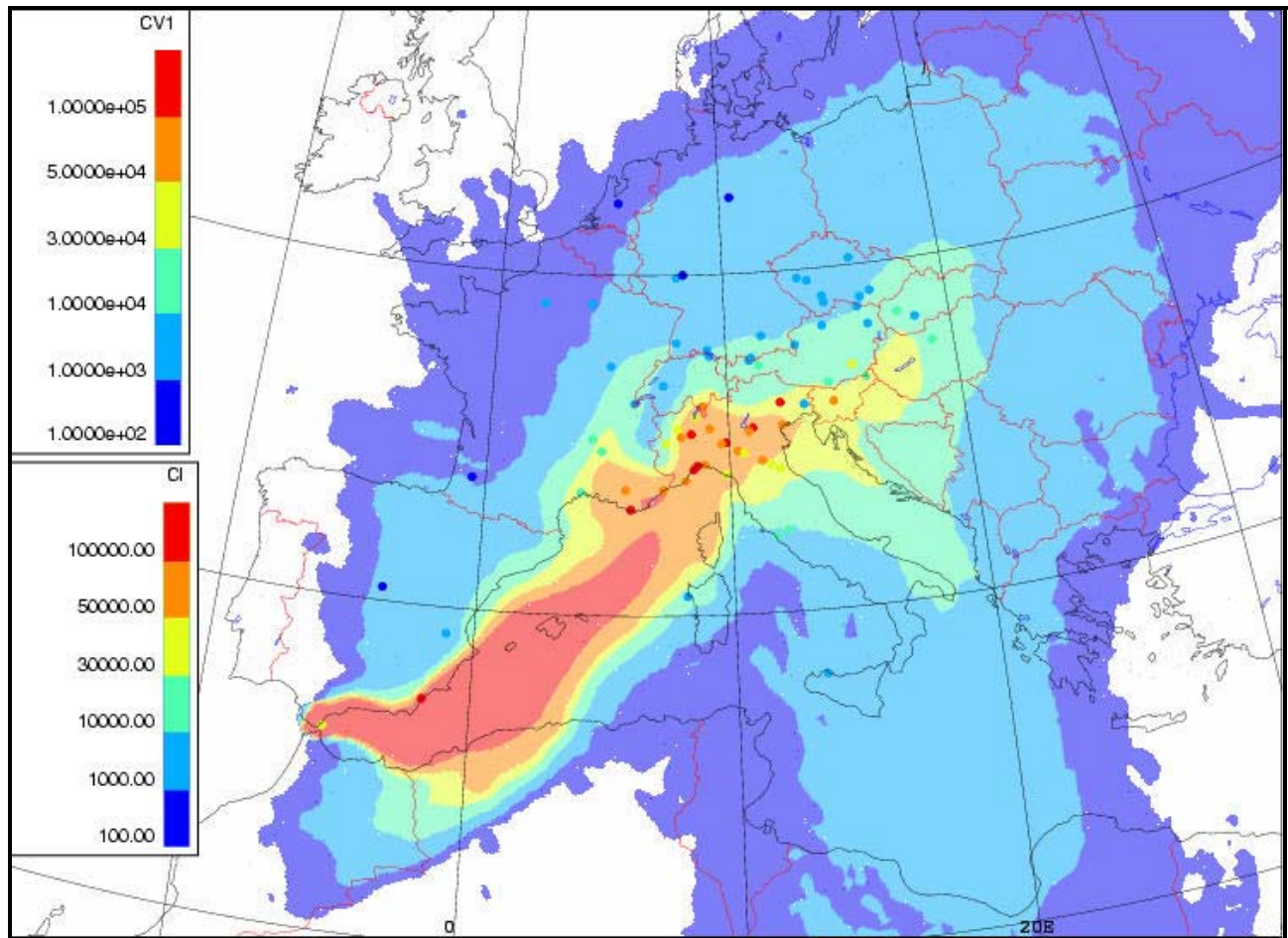


Figure 6. May 30 00UTC to June 7 00 UTC 1998 time integrated modeled plume compared to observations for Algeciras incident. Units are in $\mu\text{Bq h m}^{-3}$. Color coding of the observations is the same as for the model simulation.

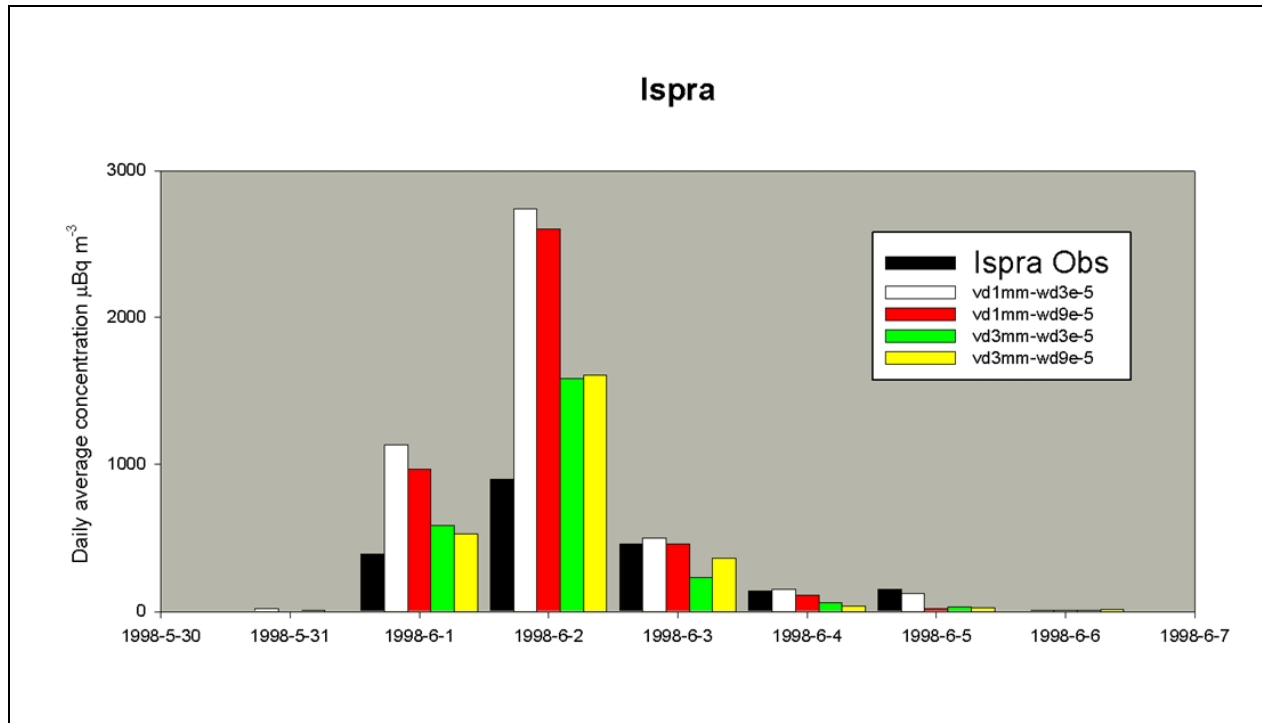


Figure 7. Time series of daily average concentration for Ispra in Northern Italy. Modeled concentrations are presented for 2 combinations of deposition velocities (1 mm/s and 3 mm/s) and 2 combinations of wet scavenging factors 3.0E-05 and 9.0E-05.

APPENDIX 1. Calculation of the vertical diffusion coefficient.

Following equation 7 of Delage (1997),

$$K_z = \frac{(kz)^2}{\phi_m \phi_h} \left| \frac{\partial \vec{U}}{\partial z} \right|$$

$$\phi_m \phi_h = \beta(1 + 12 Ri)^2 \quad Ri > 0$$

$$\phi_m \phi_h = \beta(1 - 40 Ri)^{-1/2} \quad Ri \leq 0$$

Where Ri is the gradient Richardson number. $\phi_m \phi_h$, are stability functions used in the GEM model (Mailhot et al., 1998, eqns 2.1.5 and 2.1.6). K_z is calculated at the top of first model layer above ground using this formula. This layer of thickness z_h is considered as the surface layer. At the surface (z_0) and above the ABL (H), K_z is set a low threshold K_0 . Above z_h a cubic polynomial similar to the O'Brien (1970) formula is used.

$$K_z = K_0 + \left[\frac{(H - z)}{(H - z_h)} \right]^2 \left\{ K_{z_h} - K_0 + (z - z_h) \left[\frac{(K_{z_h} - K_0)}{z_h} + 2 \frac{(K_{z_h} - K_0)}{(H - z_h)} \right] \right\} \quad z_0 \leq z \leq H$$

When H the height of the ABL is not available, it is estimated by the height at which the gradient Richardson number Ri reaches the critical value of 0.25.

APPENDIX 2. Average concentration calculation.

In the context of Lagrangian modeling, concentration is defined by the following equation

$$c(\vec{x}, t) = \int_{-\infty}^t \int_V S(\vec{x}_0, t_0) p(\vec{x}, t | \vec{x}_0, t_0) d\vec{x}_0 dt_0$$

where S is the source function, V is the 3-D domain where the source is defined, and the conditional probability that a particle is found at point (x, t) , given that it was at point (x_0, t_0) , (Sawford, 1985). Clearly the concentration c thus defined is an ensemble mean. The source function is general and can describe any function of space and time to issue particles. However in practice, particles are issued at specific points in time and space, in a discrete fashion. For one particle the source function becomes a Dirac delta function, centered on the source point, and the particle concentration becomes the conditional probability density function itself. If N particle are issued with a mass m_p , from a set of points (x_p, t_p) then the resulting particle mass concentration is :

$$c(\vec{x}, t) = \sum_{p=1}^N m_p(x, t) p(\vec{x}, t | \vec{x}_p, t_p)$$

Here we assume that m_p can change as a function of time and position, due to various processes like radioactive decay, which depends on time only, or like dry and wet deposition which depend on the particle trajectory; however changes in m_p do not affect the trajectory itself. Again $c(\vec{x}, t)$ is an ensemble mean. It also gives an instantaneous concentration at a point. In reality concentrations are measured during a certain sampling time over a certain sampling volume. Therefore an average concentration is calculated as follows:

$$\overline{c(x, t)}^{V_s \Delta t_s} = \frac{1}{V_s \Delta t_s} \int_{V_s \Delta t_s} c(\vec{x}, t) dV dt = \frac{1}{V_s \Delta t_s} \sum_{p=1}^N \int_{V_s \Delta t_s} m_p p(\vec{x}, t | \vec{x}_p, t_p) dV dt = \frac{1}{V_s \Delta t_s} \sum_{p=1}^N m \tau_p^{V_s \Delta t_s} \quad (\text{A.2.1})$$

$$m \tau_p^{V_s \Delta t_s} \equiv \int_{V_s \Delta t_s} m_p p(\vec{x}, t | \vec{x}_p, t_p) dV dt \quad (\text{A.2.2})$$

Where $m \tau_p^{V_s \Delta t_s}$ is defined as the mean mass weighted particle residence time in the sampling volume V_s during the sampling time interval Δt_s , centered at point (x_p, t_p) . $m \tau_p^{V_s \Delta t_s}$ is also an ensemble mean. The average concentration so defined is in fact the volume average of the ensemble mean mass weighted particle residence time within the sampling volume. In practice the ergodic hypothesis is used to assume that this average is equal to the average of the actual particles residence time within the sampling volume. Particles positions are sampled at discrete time intervals δt within the sampling interval Δt_s . Particles that fall in the sampling volume at the end of the given time interval are assumed to have a mass weighted residence time $m_p \delta t$, and particles outside the volume, a zero mass weighted residence time. Therefore

$$\overline{c(x, t)}^{V_s \Delta t_s} = \frac{1}{V_s \Delta t_s} \sum_{\delta t \in \Delta t_s} \delta t \sum_{p \in V_s} m_p \quad (\text{A.2.3})$$

This turns out to be the intuitively obvious method of summing up the mass of all particles within the sample volume to obtain the average concentration.

Other methods have been proposed essentially based on equation A.2.2. Indeed the validity of this equation is not restricted to source-receptor relationship, but can also form the basis to estimate the influence of a particle at position (x, t) given that it is found at position (x_p, t_p) . The problem is in the estimation of the functional form $p(x, t / x_p, t_p)$. These functions are generally referred to as density kernels. Various formulations have been proposed (de Haan, 1999) and they all have a certain degree of arbitrariness.

APPENDIX 3. Verification statistics definitions

Here O_i refers to an observed value and M_i to a modeled value

$$\bar{M} = \frac{1}{N} \sum_i M_i; \quad \bar{O} = \frac{1}{N} \sum_i O_i$$

$$BIAS = \bar{M} - \bar{O}$$

$$FB = \frac{BIAS}{.5(\bar{M} + \bar{O})}$$

NMSE normalized mean square error:

$$NMSE = \frac{1}{N} \sum_i \frac{(M_i - O_i)^2}{\bar{M} \bar{O}}; \quad \bar{M} = \frac{1}{N} \sum_i M_i; \quad \bar{O} = \frac{1}{N} \sum_i O_i$$

PC the Pearson correlation coefficient:

$$PC = \frac{\sum (M_i - \bar{M})(O_i - \bar{O})}{\sqrt{\sum (M_i - \bar{M})^2 \sum (O_i - \bar{O})^2}}$$

The global FMT, the figure of in time for all the i location and all the m time periods:

$$FMT = \frac{\sum_{i,m} \min(O_{i,m}, M_{i,m})}{\sum_{i,m} \max(O_{i,m}, M_{i,m})}$$

FA2= fraction of Modeled values within a factor of 2 of the Observed value

FA5= fraction of Modeled values within a factor of 5 of the Observed value

REFERENCES

- Boughton, B.A., Delaurentis, J.M., and Dunn, W.E., 1987, A Stochastic Model of Particle Dispersion in the Atmosphere, *Boundary-Layer Meteorology*, **40** (1-2), 147–163, [doi:10.1007/BF00140073](https://doi.org/10.1007/BF00140073).
- de Haan, P., 1999, On the Use of Density Kernels for Concentration Estimations Within Particle and Puff Dispersion Models, *Atmospheric Environment*, **33** (13), 2007–2021, [doi:10.1016/S1352-2310\(98\)00424-5](https://doi.org/10.1016/S1352-2310(98)00424-5).
- Delage, Y., 1988, A Parameterization of the Stable Atmospheric Boundary Layer, *Boundary-Layer Meteorology*, **43** (4), 365–381, [doi:10.1007/BF00121713](https://doi.org/10.1007/BF00121713).
- Delage, Y., 1997, Parameterising Sub-Grid Scale Vertical Transport in Atmospheric Models Under Statically Stable Conditions, *Boundary-Layer Meteorology*, **82** (1), 23–48, [doi:10.1023/A:1000132524077](https://doi.org/10.1023/A:1000132524077).
- Hanna, S.R., 1983, Lateral Turbulence Intensity and Plume Meandering During Stable Conditions, *Journal of Climate and Applied Meteorology*, **22** (8), 1424–1430, [doi:10.1175/1520-0450\(1983\)022<1424:LTIAPM>2.0.CO;2](https://doi.org/10.1175/1520-0450(1983)022<1424:LTIAPM>2.0.CO;2).
- Mailhot, J., Bélair, S., Benoit, R., Bilodeau, B., Delage, Y., Filion, L., Garand, L., Girard, C., and Tremblay, A., 1998, Scientific Description of RPN Physics Library, Version 3.6, *CMC Internal Publication*, <http://collaboration.cmc.ec.gc.ca/science/rpn/physics/physic98.pdf>.
- O'Brien, J.J., 1970, A Note on the Vertical Structure of the Eddy Exchange Coefficient in the Planetary Boundary Layer, *Journal of the Atmospheric Sciences*, **27** (8), 1213–1215, [doi:10.1175/1520-0469\(1970\)027<1213:ANOTVS>2.0.CO;2](https://doi.org/10.1175/1520-0469(1970)027<1213:ANOTVS>2.0.CO;2).
- Pudykiewicz, J.A. and Koziol, A.S., 1998, An Application of the Theory of Kinematics of Mixing to the Study of Tropospheric Dispersion, *Atmospheric Environment*, **32** (24), 4227–4244, [doi:10.1016/S1352-2310\(98\)00181-2](https://doi.org/10.1016/S1352-2310(98)00181-2).
- Rodean, H.C., 1996, Stochastic Lagrangian Models of Turbulent Diffusion, *AMS Meteorological Monographs*, **26** (48), ISBN 1-878220-23-3, 84 pp.
- Sawford, B.L., 1985, Lagrangian Statistical Simulation of Concentration Mean and Fluctuation Fields, *Journal of Climate and Applied Meteorology*, **24** (11), 1152–1166, [doi:10.1175/1520-0450\(1985\)024<1152:LSSOCM>2.0.CO;2](https://doi.org/10.1175/1520-0450(1985)024<1152:LSSOCM>2.0.CO;2).
- van Dop, H., Addis, R., Fraser, G., Girardi, F., Graziani, G., Inoue, Y., Kelly, N., Klug, W., Kulmala, A., Nodop, K., Pretel, J., 1998, ETEX: A European Tracer Experiment; Observations, Dispersion Modelling and Emergency Response, *Atmospheric Environment*, **32** (24), 4089–4094, [doi:10.1016/S1352-2310\(98\)00248-9](https://doi.org/10.1016/S1352-2310(98)00248-9).

Wilson, J.D., Ferrandino, F.J. and Thurtell, G.W., 1989, A Relationship Between Deposition Velocity and Trajectory Reflection Probability for Use in Stochastic Lagrangian Dispersion Models, *Agricultural and Forest Meteorology*, **47** (2-4), 139–154, [doi:10.1016/0168-1923\(89\)90092-0](https://doi.org/10.1016/0168-1923(89)90092-0).

Wilson, J.D. and Sawford, B.L., 1996, Review of Lagrangian Stochastic Models For Trajectories in the Turbulent Atmosphere, *Boundary-Layer Meteorology*, **78** (1-2), 191–210, [doi:10.1007/BF00122492](https://doi.org/10.1007/BF00122492).